JOC The Journal of Organic Chemistry

Featured Article

pubs.acs.org/joc

Fluorine End-Capped Optical Fibers for Photosensitizer Release and Singlet Oxygen Production

Dorota Bartusik, David Aebisher, Goutam Ghosh, Mihaela Minnis, and Alexander Greer*

Department of Chemistry and Graduate Center, City University of New York, Brooklyn College, Brooklyn, New York 11210, United States

Supporting Information

ABSTRACT: The usefulness of a fiber optic technique for generating singlet oxygen and releasing the pheophorbide photosensitizer has been increased by the fluorination of the porous Vycor glass tip. Singlet oxygen emerges through the fiber tip with 669-nm light and oxygen, releasing the sensitizer molecules upon a [2 + 2] addition of singlet oxygen with the ethene spacer and scission of a dioxetane intermediate. Switching from a nonfluorinated to a fluorinated glass tip led to a clear reduction of the adsorbtive affinity of the departing sensitizer with improved release into homogeneous toluene solution and bovine tissue, but no difference was found in water since the sensitizer was insoluble. High surface coverage of the nonafluorohexylsilane enhanced the cleavage efficiency by 15% at the ethene site. The fluorosilane groups also caused crowding and seemed to reduce access of $^1O_2$ to the ethene site, which attenuated the total quenching rate constant k_T, although there was less wasted $^1O_2$ (from surface physical quenching) at the fluorosilane-coated than the native SiOH silica. The observations support a quenching mechanism that the replacement of the SiOH groups for the fluorosilane C−H and C−F groups enhanced the $^1O_2$ lifetime at the fiber tip interface due to less efficient electronic-to-vibronic energy transfer.

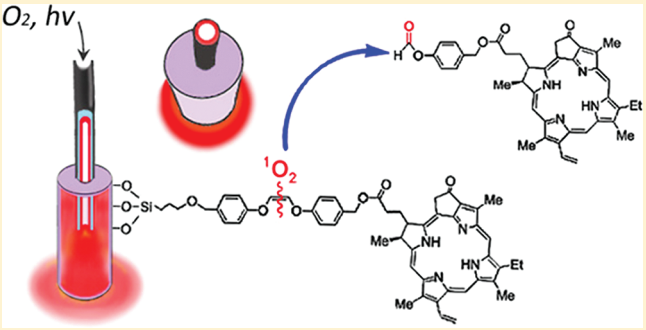

INTRODUCTION

Photodynamic therapy (PDT) methods[1] could be developed which *do not* rely on the use of intravenously injected photosensitizers to generate $^1O_2$ for the treatment of tumors *and which could* also oxygenate hypoxic tumors. One such method is the fiber optic photodetachment of sensitizer molecules, which is a relatively new organic photochemistry approach. Only two papers have been reported on the subject,[2,3] where O_2 is sparged through a porous Vycor glass tip bound to a (*Z*)-1,2-dioxyethene spacer, photo-*dis*connecting sensitizer molecules upon scission of a dioxetane intermediate (Figure 1). Dioxetanes can decompose thermally or photochemically,[4−6] and their decomposition is catalyzed by silica.[7]

The discharge of the sensitizer from the probe tip is a key event in the method. Because the sensitizer can adsorb onto the probe tip, processes to inhibit the adsorption need to be explored. Fluoroalkylsilane coatings on porous silica have repellant and self-cleaning properties,[8,9] and such a modification could be introduced into the fiber optic system to potentially enhance the sensitizer release.

Here, we report on a fluorinated fiber optic tip bound to a photolabile ethene-sensitizer to attempt to minimize adsorption of the sensitizer once the ethene bond was cleaved. Specifically, we (1) quantitated sensitizer repulsion at the fluorinated probe surface, (2) synthesized hybrid tips by covalent attachment of the pyropheophorbide-*a* monoester photosensitizer via a stable linkage to the fluorinated glass bound to the end of a hollow optical fiber, (3) determined the efficiency with which the sensitizer molecules bound to the fluorinated tips cleave free in toluene solution and bovine tissue as in vivo model surroundings, (4) quantitated the quenching of the silica surface and ethene linkage by $^1O_2$, by measuring the total bimolecular quenching rate constant k_T, and (5) utilized $^1O_2$ quenching and lifetime (τ) data for bond types in silica containing C−H and C−F bonds, particularly that replaced the SiOH bonds to identify loading and quencher parameters that influence the photosensitizer turnout yield.

RESULTS AND DISCUSSION

Fluorination of Porous Vycor Glass. We attempted to generate sensitizer repellent fiber tips by loading nonafluorohexyltrimethoxysilane (**5**) onto porous Vycor glass (Table 1). Monoliths of Vycor **6** (0.41 g) were placed into a solution of fluorosilane **5** toluene solution under mild conditions using established silane-to-silica coupling reactions.[10,11] The fluorosilane loadings ranged from 0.34 mmol (**7**), 1.16 mmol (**8**), and 1.45 mmol (**9**) to 1.60 mmol (**10**) per gram, and the tips had a noticeable yellow color and showed characteristic C−F stretching vibration bands in the infrared at 1408 cm^{-1} in the Vycor.[12] The Vycor pieces (**6**−**10**) were immersed in 10% DMSO water solutions containing

Received: March 26, 2012
Published: April 30, 2012

   dx.doi.org/10.1021/jo3006107 | J. Org. Chem. 2012, 77, 4557−4565

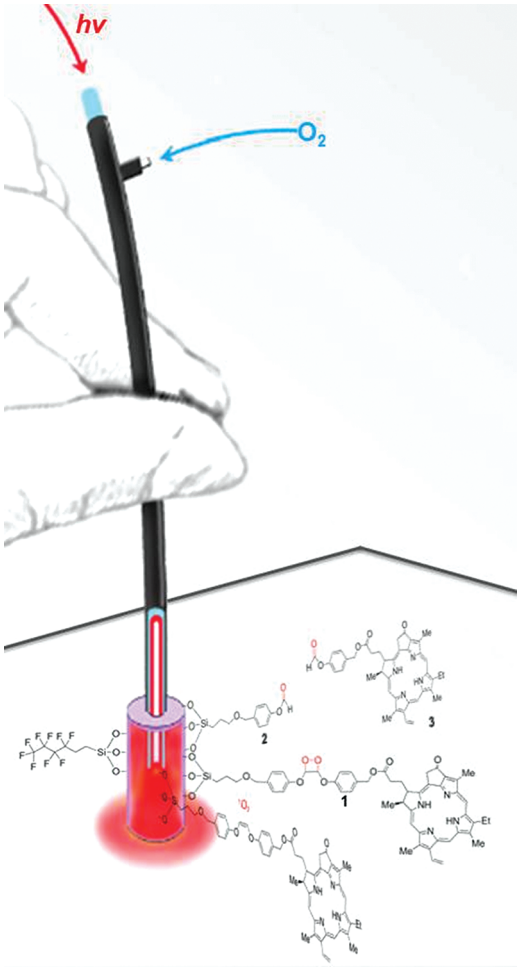

Figure 1. Schematic of the fluorinated fiberoptic probe tip showing sensitizer release **3** and remnant fragment **2** after scission of dioxetane **1** that arose from a [2 + 2] addition of singlet oxygen to the ethene bond. The attached nonafluorosilane group is shown, as is as a cutaway view of the hollow fiber core. Visible light and O_2 were delivered through the fiber to the tip causing the photodetachment and the adsorption of the sensitizer molecules.

pyropheophorbide-*a* **4** (Scheme 1), which was used as a model compound for the pheophorbide derivative **3** that actually

Scheme 1

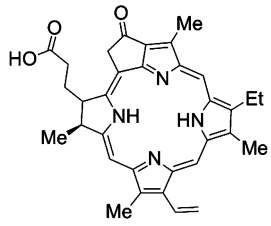

4

departs from the optical fiber. The fluorosilane coatings improved the sensitizer repellent properties, e.g., compare Vycors **6** and **10** (entry 9), which led to a decrease in the adsorption from 87% to 9.2%. The adsorption was a time-dependent process, for Vycor **10**, the adsorption of **4** reached 1.7% after 30 min and 9.2% after 4 h.

Synthesis of the Hybrid Glasses. Next, syntheses were carried out which bonded fluorosilane **5**, sensitizersilane **13**, and/or ethenesilane **14** to the Vycor glass surface, producing functionalized Vycors **15**–**18** (Scheme 2). The reaction required ethene "spacer" group **11**, which was synthesized from a known procedure[2] and reacted with **4**, EDC, and DMAP, producing the pheophorbide monoester **12**. Vycors **6** or **10** were used, along with (3-iodopropyl)trimethoxysilane to couple the sensitizer **13** or the ethene **14** to the surface. Vycor **15** was known from previous work,[2] and had been characterized by FT-IR and UV–vis spectroscopy, where the sensitizer was thinly coated and reached a penetration depth of 0.08 mm into the glass. The absorption spectra of **15** and **16** were identical to within experimental error, with no shifting or broadening of the Soret (414 nm) and Q-absorption (666 nm). The amount of fluorosilane **5**, sensitizersilane **13**, and ethenesilane **14** loaded onto the Vycor was 1.60 mmol, 400 nmol, and 400 nmol per gram, respectively.

The calculated spatial separation distances of silanol and silanes arrayed on the Vycor surfaces is shown in Table 2. In 10, fluorosilane is ~1.1 nm long and when orthogonal to the surface is separated from other fluorosilanes by ~1.2 nm. In **15**, the sensitizersilane is ~3.2 nm long and when orthogonal to the surface is separated from other sensitizersilanes by 64 nm. Spatial separation distances were also estimated for **17** and **18**. The covalent connections, including CH_2 bridges, are flexible

Table 1. Nanomoles and Percent Adsorption of Pyropheophorbide-*a* 4 onto Native and Fluorinated Vycor Surfaces in 10% DMSO Water[a]

entry[b,c]	time (h)	Vycor **6** nmol (and %) adsorbed **4**	Vycor **7** nmol (and %) adsorbed **4**	Vycor **8** nmol (and %) adsorbed **4**	Vycor **9** nmol (and %) adsorbed **4**	Vycor **10** nmol (and %) adsorbed **4**
1	0	0 (0)	0 (0)	0 (0)	0 (0)	0 (0)
2	0.5	20 (11.7)	12 (7.0)	11 (6.5)	11 (6.5)	3 (1.7)
3	1.0	36 (21.1)	12 (7.0)	11 (6.5)	11 (6.5)	5 (2.9)
4	1.5	40 (23.5)	13 (7.6)	12 (7.0)	16 (9.4)	6.5 (3.9)
5	2.0	42 (24.7)	13 (7.6)	28 (16.4)	16 (9.4)	8 (4.9)
6	2.5	98 (57.6)	64 (37.6)	28 (16.5)	17 (10)	11.3 (6.9)
7	3.0	100 (58.8)	67.5 (39.7)	43 (25.3)	17 (10)	12 (7.4)
8	3.5	108 (63.5)	77.2 (45)	43 (25.3)	18 (10.5)	14.2 (8.7)
9	4.0	148 (87)	99 (58)	50 (30)	19 (11.7)	15 (9.2)

[a]Dissolution of **4** required the addition of DMSO to water. Adsorption of **4** onto native or fluorinated Vycor samples, which were followed at λ = 416 nm. The Vycor samples were immersed in 10% DMSO water (2.0 mL), which contained **4** (10 mM). The Vycor samples were removed at the indicated times. [b]Native Vycor **6**. [c]Fluorosilane **5** loadings onto the Vycor ranged were 0.34 mmol (**7**), 1.16 mmol (**8**), 1.45 mmol (**9**), to 1.60 mmol (**10**) per gram.

dx.doi.org/10.1021/jo3006107 | *J. Org. Chem.* 2012, 77, 4557–4565

Scheme 2. Synthesis of Fluorosilane, Sensitizersilane, and Ethenesilane Functionalized Vycors 15−18[a]

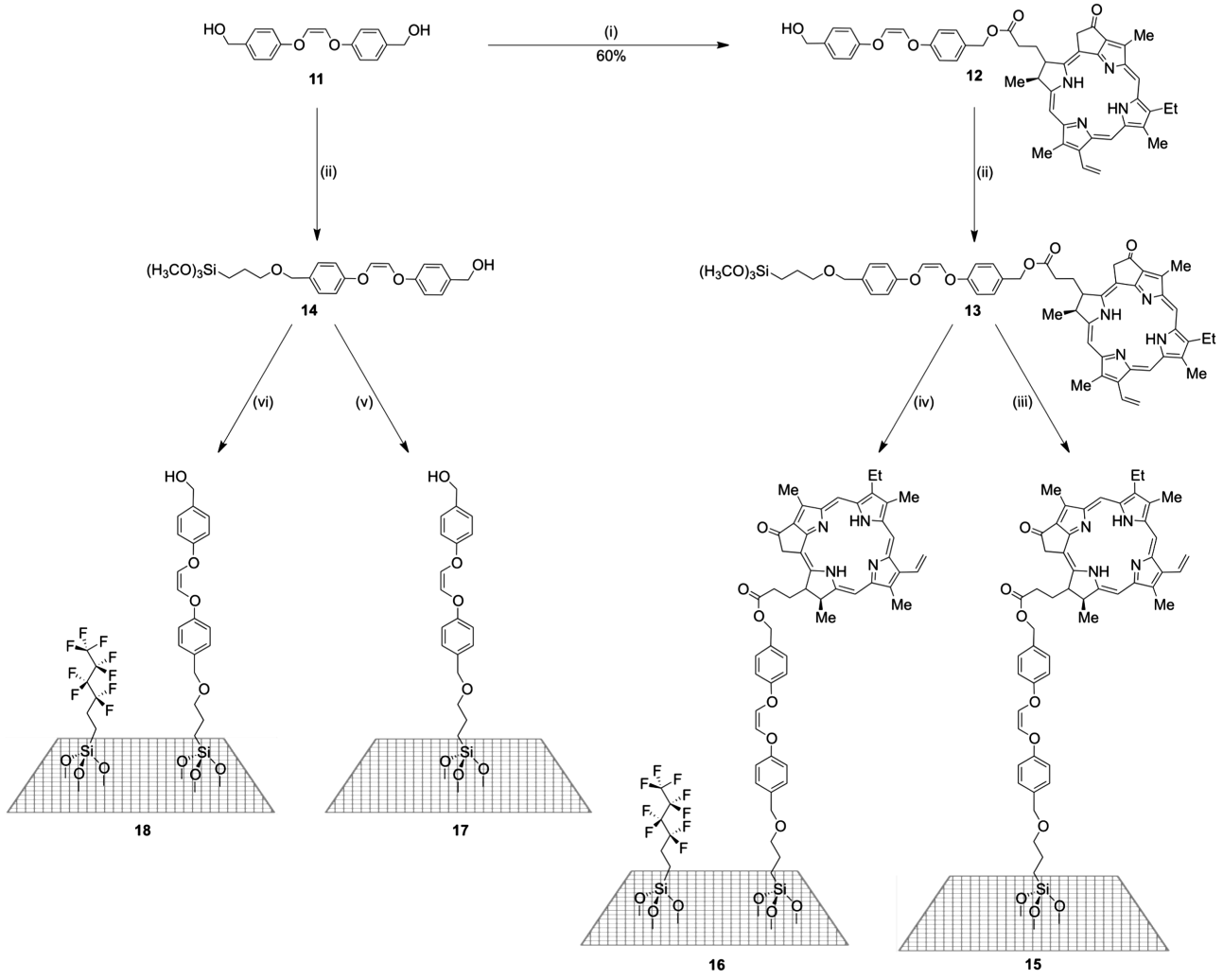

[a]Reagents and conditions: (i) pyropheophorbide-*a* **4**, EDC, DMAP, CH_2Cl_2, 25 °C, 24 h; (ii) $(CH_3O)_3SiCH_2CH_2CH_2I$, NaH, THF, under N_2, 70 °C, 24 h; (iii) native Vycor **6**, 0.4 g of monoliths (predried at 500 °C), toluene, reflux 110 °C, 24 h; (iv) fluorosilane-functionalized Vycor **10**, 0.4 g of monoliths (predried at 350 °C), toluene, reflux 110 °C, 24 h; (v) native Vycor **6**, 60 μm particles (predried at 500 °C), toluene, reflux 110 °C, 24 h; (vi) Vycor **10**, 60 μm particles (predried at 350 °C), toluene, reflux 110 °C, 24 h.

due to *gauche* and *anti* conformations, and the orientations of the surface-mounted silanes are uncertain. It seems possible that the orthogonal position of the dye relative to the surface is higher populated due to the fluorosilane congestion. UV−vis and solid state MAS NMR spectroscopy[13,14] have yet provided sparingly little information on the conformations of silanes in silica; however, the noncovalent interactions between the fluorosilane and the sensitizer sites was probable due to the 1.2 nm proximity to each other, with even more intrasurface interactions when extended horizontally toward each other.

From a photochemical point of view, **15** and **16** possess strong absorptions that overlap the 669 nm diode laser line providing an efficient means of dye excitation and generation of $^1O_2$. As will be seen later, Vycors **17** and **18** lacking the sensitizer head were required for the k_T measurements to assess the reactivity of $^1O_2$ at the ethene sites (vide infra). Next, we determined the extent to which sensitizer **3** cleaved free from fiber tips **15** and **16**.

Sensitizer Photorelease via the Fiber Probe Tip. Vycor probe tips **15** or **16** were affixed to the hollow fiber optic, where O_2 flowed and diode laser light were delivered through the tip (~0.2 ppm O_2/min; irradiance 4.8 mW cm^{-2}). Electron-rich alkenes can cleave apart by visible-light sensitized $^1O_2$ reactions,[15−18] although their use in sensitizer drug delivery, as described in this paper, is rather uncommon.[19,20] We find the ethene spacer group of **15** and **16** was photooxidized and led to the release of sensitizer **3**. Control experiments showed no detachment of sensitizer molecules in the absence of light and oxygen, which demonstrated the photooxidation requirement.

Shown in Figure 2 is the amount of sensitizer **3** released into in toluene-d_8 to assess the fluorine-probe tip effects for repelling sensitizer upon photocleavage. Of the ethene bonds broken, high amounts of **3** remained adsorbed onto nonfluorinated probe tip **15** (87%). However, **16** was superior and the amount adsorbed was only 0.9% of the ethene bonds that were broken, demonstrating the repellent property of the fluorinated probe tip in toluene. Aprotic media such as toluene was needed because in aqueous solution, ~100% retention of the sensitizer occurred with both **15** and **16** on the tip surface, due to dye insolubility. To further assess fluorine-surface effects, the sensitizer photocleavage was quantitated in bovine tissue.

dx.doi.org/10.1021/jo3006107 | J. Org. Chem. 2012, 77, 4557−4565

Table 2. Nanometer Distances Separating SiOH, Fluorosilane, Sensitizersilane, and Ethenesilane Sites on the Vycor Samples[a]

Vycor **10**		
	SiOH	fluorosilane
SiOH	1.0	1.0−1.2
fluorosilane	1.0−1.2	1.2
Vycor 15		
	SiOH	sensitizersilane
SiOH	1.0	1.2
sensitizersilane	1.2	64.0
Vycor 16		
	SiOH	fluorosilane	sensitizersilane
SiOH	1.0	1.0−1.2	1.2
fluorosilane	1.0−1.2	1.2	1.2
sensitizersilane	1.2	1.2	64.0
Vycor 17		
	SiOH	ethenesilane
SiOH	1	1.2
ethenesilane	1.2	64.0
Vycor 18		
	SiOH	fluorosilane	ethenesilane
SiOH	1.0	1.0−1.2	1.2
fluorosilane	1.0−1.2	1.2	1.2
ethenesilane	1.2	1.2	64.0

[a]Nearest neighbor distances and surface coverage were calculated as described in the Experimental Section.

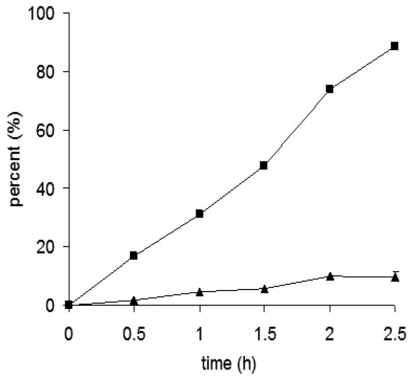

Figure 2. Percent of sensitizer **3** photoreleased from the fiber optic delivering light and oxygen to probe tip **15** (black triangles) and to probe tip **16** (black squares) in toluene-d_8 at 26 °C.

Table 3 shows that sensitizer photorelease in bovine tissue was improved by ∼11% for probe tip **16**, compared to **15**. The detection of **3** in the pigmented tissue was conducted with fluorescence microscopy, and any sensitizer mass remaining on the probe surface was dissociated by methanol Soxhlet extraction. If there is maneuvering of the probe tip, sensitizer discharge can also occur by mechanical action, but this type of release effect remains to be fully tested.

All experiments were carried out at room temperature, 26 °C. The fiber tip receiving the 669 nm light did not increase the temperature of surrounding toluene over time, wherein temperature-dependent solvent quenching of singlet oxygen becomes important.[21] Diminished singlet oxygen rates would have been expected of entropy-controlled $^1O_2$ reactions of the ethene at elevated temperatures.[22−25]

The results showed the yield of the ethene bond photocleavage was greater in **16** (90.7%) compared to **15** (75.6%) after 2.5 h. The difference in the photocleavage percent yield between **15** and **16** was real, but it was not possible to measure the chemical rate constant (k_r) of $^1O_2$ with ethene bound to the glass since comparative kinetics with a homogeneous trap[26] is probably invalid. The mass percent of fluorosilane in **10** and **16** (52%) was far greater than that of the sensitizersilane in **16** (0.03%) (Table 4), where the fluorosilane coated Vycor always

Table 4. Mass Percent of Silanol, Fluorosilane, Sensitizersilane, and Ethenesilane of the Vycor Tips

Vycor	mass % fluorosilane	mass % sensitizersilane	mass % ethenesilane	mol fraction
10	52	0	0	0.96
15	0	0.03	0	0.02
16	52	0.03	0	0.96
17	0	0	0.01	0.02
18	52	0	0.01	0.96

enhanced the photooxidation efficiency (Table 3). Somewhat similarly, a fluorous biphasic catalytic reaction was reported to enhance photooxidation efficiency of $^1O_2$ in supercritical CO_2.[27] An intriguing finding by Scaiano et al. was the detection of $^1O_2$ within zeolites, and $^1O_2$ which escaped and entered the bulk media.[28] Enhanced $^1O_2$ lifetimes have been found within fluorinated zeolites[29] due to decreased quenching compared to nonfluorinated zeolites,[30,31] which led us to measure the rate constants of singlet oxygen with the fluorinated and nonfluorinated Vycor surface and with the ethene sites in the porous glass.

Rates of the Singlet Oxygen Reactions. Table 5 shows the total rate constants (k_T) of $^1O_2$ with 60 μm sized Vycor particles **6**, **10**, **17**, and **18** from monitoring the quenching of its

Table 3. Yields of Sensitizer 3 Photoreleased and Adsorbed by Probe-Tip Photooxidation[a−c]

entry	Vycor probe tip	medium	photoreleased **3** (%)	photoreleased **3** (nmol)	adsorbed **3** (%)	adsorbed **3** (nmol)
1	**15**	toluene-d_8	9.6 ± 1.8[c]	8.6 ± 1.6	66.1 ± 8.6	59.5 ± 7.7
2	**16**	toluene-d_8	88.6 ± 0.8[c]	77.9 ± 0.7	0.8 ± 0.1	1.0 ± 0.5
3	**15**	bovine	2.2 ± 0.6	2.0 ± 0.4	68.9 ± 2.3	62 ± 3
4	**16**	bovine	13.0 ± 4.0	12.7 ± 3.9	63 ± 5	55.4 ± 1.9

[a]Internal irradiation of tip via a fiber optic connected to the 669-nm diode laser and operated at 4 psi O_2 pressure, 0.2−0.3 ppm/min O_2 flow rate through the probe tip. After 2.5 h, fluence through tip = 43 J/cm^2. Fiber tip dimensions: cylinder shape with a length of 8.0 mm, diameter of 5.0 mm, and hole (2.0 length 3.0 mm diameter). Experiments were repeated three or more times. [b]Absorption spectroscopy was used for the quantitation of **3** in toluene-d_8 (1.0 mL). Fluorescence microscopy was used to detect **3** in the bovine tissue. [c]Soxhlet extraction was used to determine the percent of ethene bonds photooxidatively cleaved in **15** and **16** (average of 4 experiments each).

dx.doi.org/10.1021/jo3006107 | J. Org. Chem. 2012, 77, 4557−4565

Table 5. k_T Measurements for the Reaction with Singlet Oxygen by 6, 10, 17, and 18 Particles in Toluene-h_8[a]

entry	sample	k_T (L g^{-1} s^{-1})
1	Vycor **6**	21.7 ± 3.6
2	Vycor **10**	15.1 ± 2.2
3	Vycor **17**	53.0 ± 5.2
4	Vycor **18**	37.0 ± 6.1

[a]Heterogeneous mixture of 60-μm Vycor particles in toluene. Average of three experiments carried out at 26 °C.

time-resolved emission at 1270 nm in toluene. Oxygen sparging caused O_2 diffusion into the porous glass particles, which were stirred with a microstir bar during the pulsed 355 nm irradiation. Other research groups have reported on O_2 diffusion into porous glass and protein matrices for sensitization by embedded dyes[32] and residues.[33]

Here, k_T values were not determined for the Vycor monoliths due to difficulties assessing effects to the outer 0.08 mm layer of the glass, where the silanes attached. It was assumed that the Vycor particles and monoliths bore similar reflective properties.[34] Various substrate concentrations are needed to construct k_T plots;[35,36] for our heterogeneous mixtures, various weights of the Vycor particles were used (Figure 3).

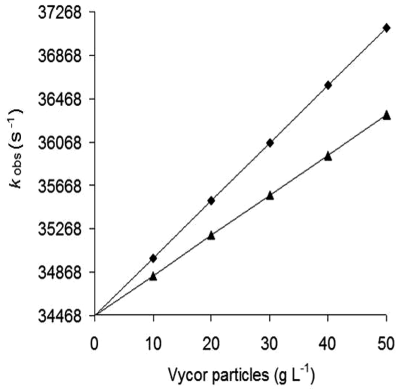

Figure 3. Total rate constant (k_T) plots of $^1O_2$ obtained by monitoring the 1270 nm signal by adding various quantities of ethene-bonded particles **17** (black diamonds) and ethene-bonded fluorinated particles **18** (black triangles) into toluene-h_8 at 25 °C.

The k_T for $^1O_2$ removal by fluorinated Vycor **10** was decreased compared to native Vycor **6** (entries 1 and 2, Table 5). This was attributed to a lower number of higher quenching O−H oscillators in **6** that were exchanged for a higher number of lower quenching C−H and C−F oscillators in **10**. Shown in Table 6 is that 96% of the 1×10^{20} SiO−H bonds of native Vycor **6** were supplanted with 3.8×10^{21} and 6.7×10^{21} new C−H and C−F bonds in **10**, where the net effect was one of reduced $^1O_2$ quenching at the silica/toluene interface. We assumed a quenching mechanism of electronic (E)→vibronic (V) exchange energy transfer from $^1O_2$ by the SiO−H, C−H, and C−F groups, where quenching efficiency decreases in the order: O−H > C−H > C−F.[37−41] The rates of $^1O_2$ deactivtion by solvated molecules is expected to be increased from molecules mounted in a silica matrix, and in the fluid phase, lifetimes of $^1O_2$ are known to increase in the order: protic solvents < alkane solvents < fluorinated solvents, consistent with E→V energy transfer rather than dipole−dipole energy transfer.[42] C−H vibrational deactivation can be accompanied by charge-transfer complexation in some cases as with $^1O_2$ and cubanes.[43]

Equal concentrations of sensitizer **4** were used in the heterogeneous mixtures because the sensitizer can act as a quencher and the lifetime of $^1O_2$ (τ) depends on the its concentration.[37] Thus, Vycors **17** and **18** were used because they lacked the sensitizer heads of **15** and **16**. We found the k_T of $^1O_2$ for the surface-bound ethene was decreased by ∼1.4-fold for fluorinated **18** compared to nonfluorinated **17**. Because the packing density is increased in **18** (Table 3), the fluorosilane groups probably have reduced $^1O_2$ access to the ethene site. Nevertheless, the efficiency for ethene bond cleavage (described earlier) was increased with the fluorinated silica surface, increasing the amount of the sensitizer released from the probe tip. Clennan and Chen[44] measured k_T values of ∼28−36 L g^{-1} s^{-1} for sulfides mounted onto 30 μm porous silica particles, which were slightly smaller than those for **17** and **18** (Table 5). The increased k_T values for **17** and **18** were expected because dialkoxyethenes are similar to ∼2-fold greater than alkyl sulfides in homogeneous solution.[45]

Mechanistic Considerations. After diffusion of O_2 through the silica where it was sensitized by the attached dye (Figures 1 and 4), singlet oxygen reacts with the ethene site resulting in a surface-bound dioxetane. The scission of the dioxetane leads to sensitizer release into the surrounding media *or* adsorption onto the silica surface. We found that (i) the more the Vycor tip was fluorinated, the lower the adsorption of the hydrophobic sensitizer **3**, where improved probe tip repulsion due to fluorination was seen in toluene and bovine tissue, but not in water where the dye was insoluble. In mammalian PDT, it is generally desired that the sensitizer is hydrophobic (usually to a large extent) to facilitate uptake by cells and localization in the lipid bilayer.[46,47] (ii) Singlet oxygen quenching by the fluorinated Vycor surface was decreased compared to the native SiOH-coated Vycor. This was clearly due to physical quenching since the glasses were not photooxidized. (iii) Table 3 shows that the fluorinated fiber tip increased the reactivity of the ethene bond, the ethene bond cleavage yield was 91% in the fluorinated tip, and 76% in the

Table 6. Absolute Number of Bond Types of Surface Vycors per Gram

Vycor	SiO−H[a]	C−H	C−F	C−C[b]	C−O[b]	C−N[b]
6	1.0×10^{21}					
10	3.6×10^{19}	3.8×10^{21}	6.7×10^{21}	3.8×10^{21}		
15	9.9×10^{20}	1.2×10^{19}		1.1×10^{19}	1.8×10^{19}	1.8×10^{18}
16	3.6×10^{19}	3.8×10^{21}	6.7×10^{21}	3.8×10^{21}	1.9×10^{18}	1.9×10^{18}
17	9.9×10^{20}	4.8×10^{18}		4.1×10^{18}	1.7×10^{18}	
18	3.6×10^{19}	3.8×10^{21}	6.7×10^{21}	3.8×10^{21}	1.7×10^{18}	

[a]Bond types within the silica particles or within the monoliths at a penetration depth of 0.08 mm. [b]Not restricted to single bonds.

dx.doi.org/10.1021/jo3006107 | J. Org. Chem. 2012, 77, 4557−4565

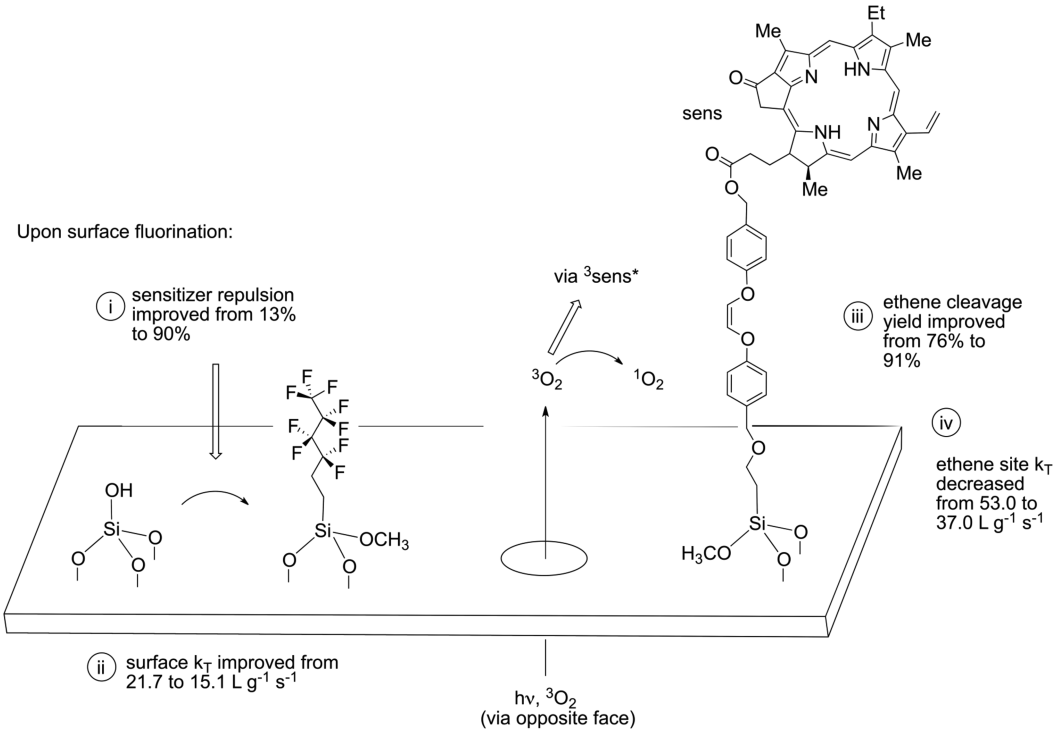

Figure 4. Mechanistic summary of photosensitized oxidation at the probe tip interface via the bottom-up production of $^1O_2$ through the core of the hollow optical fiber.

nonfluorinated tip, whereas (iv) the k_T of $^1O_2$ for quenching the surface-bound ethene decreased by ∼1.4 fold with fluorinated **18** compared to nonfluorinated **17**.

In summary, there is reduced physical quenching of $^1O_2$ at the fluorosilane-coated site compared to the native SiOH silica. But there are competitive paths at the ethene site due to fluorination of the glass, one enhancing chemical quenching and the other slowing total quenching. With a longer $^1O_2$ lifetime at the fluorinated tip/solution interface, the enhanced ethene cleavage is attributed to more efficient chemical quenching (although k_r was not measured since it is a heterogeneous system). In parallel, steric hindrance from the fluorosilane chains seems to reduce access to the ethene sites, which attenuated the total rate constant k_T value.

CONCLUSION

The silica matrix tip of an optical fiber was modified to improve the release of a PDT-type pheophorbide sensitizer, where mechanistic questions were probed with organic photochemistry. The fluorinated optical fiber tip led to decreased adsorptive affinity of the sensitizer, and some quenching properties that were advantageous, including reduced physical quenching of $^1O_2$ by the fluorosilane-coated than the native SiOH surface, and enhanced chemical quenching of the ethene site bonding the sensitizer to the probe tip. It could be argued that the postphotocleavage adsorption step was diminished from the dye favoring an orthogonal position due to the fluorosilane congestion on the surface.

Our conclusion is that the fluorinated fiber system described here is appropriate for dye release studies in in vitro and tissue PDT experiments. While there is value for research in precise tumor removal [especially when the tumor is adjacent to vital tissue (near-neighbor effect)] and for the oxygenation of hypoxic tumor sites, the question is what technology can be developed to make significant inroads. Current human PDT methods intravenously inject sensitizers into patients, where near-neighbor effects always present a challenge. Moreover, there is no available means to oxygenate hypoxic tumor sites[48] (save hyperbaric oxygenation methods)[49] for $^1O_2$ production, which is the main species for tumor destruction in PDT.[50]

Future fiber optic designs could include (i) a PEGylated sensitizer system to transit off of the fluorinated probe and partition better into aqueous biological media. A PEGylated polymer chlorin e_6 of Hamblin, Hasan et al.[51] was shown to be phototoxic in their PDT study of ovarian cancer cells. Since the silica matrix tip is tailorable, departure of a PEGylated sensitizer could be advantageous and will require a modified synthetic route to that presented here. (ii) In view of the temperature dependence of entropy-controlled $^1O_2$ attack on ethenes,[22−24] a probe tip whose temperature can be lowered would be expected to increase the photocleavage yield. However, very low temperatures (such as −100 °C) would not be available to exploit such entropy-control, and even temperatures below 0 °C would lead to an ice-encrusted probe tip in a biological setting whose shell could hinder the sensitizer photorelease.

EXPERIMENTAL SECTION

General Information. Methanol, 1-octanol, toluene, dichloromethane, 2,2,2-trifluoroethanol, toluene-d_8, deuterium oxide-d_2, chloroform-d_1, THF, hydrofluoric acid, magnesium sulfate, sodium hydride, (3-iodopropyl)trimethoxysilane, pyropheophorbide-*a* **4**, and 3,3,4,4,5,5,6,6,6-nonafluorohexyltrimethoxysilane **5** were obtained from commercial suppliers. Porous Vycor glass **6** was dried at 500 °C and used as 5 × 12 mm^2 monolith pieces (∼0.4 g) or as a fine powder of 60 μm particles obtained after grinding and sieving. Holes (1.5 mm diameter × 6.0 mm length) were bored into the Vycor monoliths with a Dremel drill. Compounds **11** and **12** were prepared according to a literature procedure.[2] Silanes **13** and **14** were formed in situ and were not characterized. Deionized water was purified using a deionization system. Proton NMR data were recorded at 400 MHz,

dx.doi.org/10.1021/jo3006107 | J. Org. Chem. 2012, 77, 4557−4565

carbon NMR data were collected at 100.6 MHz, and fluorine NMR data were recorded at 188.23 MHz.

Fiberoptic Technique. A device was used as described previously,[3] with a continuous wave diode laser (669 nm, 506 mW, 2.5 A output) connected to a custom-made fiber-optic cable whose distal end had a stainless steel ring where the porous Vycor caps were glued with ethyl cyanoacrylate. The laser was connected to the proximal end of the fiber through an SMA connector. The fiber optic used was 3 ft in length and had a Teflon gas flow tube running from the distal end to a T-valve surrounded by ∼60 excitation fibers randomized in a ring around it and was encased in a polyvinyl chloride jacket, which delivered 0.5 mW out of the end of the fiber. Gas flowed from a compressed oxygen gas tank and subsequently to the T-valve in the hollow fiber. The O_2 pressure was increased from 1 PSI to 4 PSI within the fiber, at which point a steady ∼0.2 ppm/min O_2 flow rate resulted through the probe tip.

Silica Dissolution by HF Treatment. A literature HF treatment method was used to dissolve the functionalized silicas and assist in their characterization by liberating the immobilized molecules from the surfaces.[52,53] Silica **10** or **15**−**18** (100 mg) in 2 mL of distilled water was added to 2 mL of 40% aqueous HF with stirring in a Teflon container at 0 °C. Dissolution of the silica occurred after ∼1 h, after which the mixture was added to 2 mL CH_2Cl_2 with stirring for 15 min at 0 °C. The organic layer was decanted and dried with anhydrous magnesium sulfate and then filtered and analyzed as a homogeneous sample[13] by GC/MS, LCMS, and ^{1}H, ^{13}C, and ^{19}F NMR spectroscopy. The HF treatment led to the decomposition of the porphyrin in the liberated molecules.

GC/MS Instrumentation and Analysis. Samples were collected in the EI mode. The capillary column was a VF-5 30 m × 0.25 mm × 0.25 μm. The solvent delay was set to 3 min, and the temperature program was 80 °C (0−5 min), 80−250 °C (5−22 min, with a rate 10 °C/min), 250 °C (22−35 min). The instrument parameters included an injector temperature of 200 °C, column flow rate of 1 mL/min.

LCMS Instrumentation and Analysis. A TOF mass spectrometer was used that wast attached to an HPLC, binary pump, and diode array detector. A 2.1 mm × 30 mm SB-C18 column was used with H_2O containing 0.1% formic acid and 5 mM ammonium formate (solvent A) and methanol containing 0.1% formic acid and 5 mM ammonium formate (solvent B) at a flow rate 0.5 mL/min. A gradient program was used: 15−85% B (0−13 min), 85% B (2 min), 85−15% B (1 min).

Fluorinated Glass 7−10. Twelve pieces of Vycor (ea. 0.41 g) were soaked in 1 × 10^{-3} M **5** (0.03 mmol), 0.43 M **5** (12.9 mmol), 0.53 M **5** (15.9 mmol), or 0.6 M **5** (18 mmol) where each batch was refluxed in toluene (30 mL) for 24 h, which led to Vycors **7**−**10**. Any **5** that was not covalently attached to the Vycor surface was washed away by Soxhlet extraction in methanol for 24 h. The ^{19}F NMR signal reduction intensity of **5** in solution was used to deduce the quantity loaded onto the glass. No fluorosilane leaching was observed from the solids after Soxhlet extraction in methanol. FT-IR (λ, cm^{-1}): 4000−3500, 3030, 2960, 2483, 1730, 1408, 1254, 1080. UV (λ, air): transparent. Anal. Calcd: C, 0.576; H, 0.030; F, 0.152. Found: C, 0.5805; H, 0.0525; F, 0.150. After dissolution of solid **10** by the HF treatment, evidence suggested that $CF_3CF_2CF_2CF_2CH_2CH_2SiF_3$ (**A**) was liberated: GC/MS (EI+) calcd for $C_6SiH_4F_{12}$ = 332 g/mol, found 332 *m/z*, t_R =5.59 min. MS (EI): 332 (M), 247 (M − SiF_3), 233 (M − CH_2SiF_3), 219 (M − $CH_2CH_2SiF_3$), 169 (M − $CF_2CH_2CH_2SiF_3$), 119 (M − $CF_2CF_2CH_2CH_2SiF_3$), 69 (M − $CF_2CF_2CF_2CH_2CH_2SiF_3$). Molecular peak ($C_6SiH_4F_{12}$, M = 332) isotopic ratio (calcd, found): [M + 1] 333 (11.4, 11.6), [M + 2] 334 (3.8, 3.9), and [M + 3] 335 (0.2, 0.2). LCMS (+ESI): calcd for $C_6SiH_4F_{12}$ = 332.16, found 331.21, t_R =12.41 min. ^{1}H NMR ($CDCl_3$, 400 MHz): 0.87 (t, $^2J_{^1H-^{19}F}$ = 46.7 Hz, $^3J_{^1H-^{19}F}$ = 0.4 Hz, 2H), 2.14 (m, $^3J_{^1H-^{19}F}$ = 46.7 Hz, $^4J_{^1H-^{19}F}$ = 0.4 Hz, 2H). ^{13}C NMR ($CDCl_3$, 100 MHz): 25.62, 51.36, 117.50, $^1J_{^{13}C-^{19}F}$ = 164.8 Hz, $^2J_{^{13}C-^{19}F}$ = 18.3 Hz, $^3J_{^{13}C-^{19}F}$ = 6.2 Hz, 117.90, $^1J_{^{13}C-^{19}F}$ = 164.8 Hz, $^2J_{^{13}C-^{19}F}$ = 18.3 Hz, $^3J_{^{13}C-^{19}F}$ = 6.2 Hz, 118.30, $^1J_{^{13}C-^{19}F}$ = 164.8 Hz, $^2J_{^{13}C-^{19}F}$ = 18.3 Hz, $^3J_{^{13}C-^{19}F}$ = 6.2 Hz, 118.50, $^1J_{^{13}C-^{19}F}$ = 164.8 Hz, $^2J_{^{13}C-^{19}F}$ = 18.3 Hz, $^3J_{^{13}C-^{19}F}$ = 6.2 Hz. ^{19}F NMR (188 MHz): −81.30 (3F), −112.57 (2F), −116.30 (2F), −124.15 (2F), −125.16 (3F).

Pheophorbide-Modified Glass 15. Vycor **15** was prepared according to a previously reported procedure.[2] Any silanes that were not covalently attached to the Vycor surface were washed by Soxhlet extraction with methanol for 24 h. Vycor **15** was stable in the dark, the sensitizer did not leach off to any measurable extent after washing with toluene or ethanol, or after Soxhlet extraction with methanol. In **15**, the ratio of SiOH to sensitizer groups was ∼100:0.02. FT-IR (λ, cm^{-1}): 4000−3500, 3080, 2970, 2420, 1750, 1360, 1200, 1055. UV (λ, air): 414 nm, 666 nm. Anal. found: C, 0.79; H, 0.034; N, 0.10. Anal. Calcd: C, 0.24; H, 0.020; N, 0.040. After dissolution of solid **15** by the HF treatment, evidence suggested that (*Z*)-$HOCH_2C_6H_4OCH{=}CHOC_6H_4CH_2OCH_2CH_2CH_2Si(OH)_3$ (**B**) was liberated: GC/MS (EI+) calcd for $C_{19}SiH_{23}O_7$ = 391, found 391, t_R = 8.92 min. MS (EI): 391 (M), 312 (M − SiO_3H_3), 270 (M − $SiO_3H_2CH_2CH_2CH_2$), 254 (M − $SiO_3H_2CH_2CH_2CH_2O$), 240 (M − $SiO_3H_2CH_2CH_2CH_2CH_2O$-$CH_2$), 164 (M − $SiO_3H_2CH_2CH_2CH_2OCH_2C_6H_4$), 148 (M − $SiO_3H_2CH_2CH_2CH_2OCH_2C_6H_4O$), 122 (M − SiO_3H_2-$CH_2CH_2CH_2OCH_2C_6H_4OCH{=}CH$), 106 (M − SiO_3H_2 $CH_2CH_2CH_2OCH_2C_6H_4OCH{=}CHO$), 30 (M − $SiO_3H_2CH_2$-$CH_2CH_2OCH_2C_6H_4OCH{=}CHOC_6H_4$), 16 (M − $SiO_3H_2CH_2$-$CH_2CH_2OCH_2C_6H_4OCH{=}CHOC_6H_4CH_2$). Molecular peak ($C_{19}SiH_{23}O_7$, M = 391) isotopic ratio (calcd, found): [M + 1] 392 (26.2, 26.1), [M + 2] 393 (3.7, 3.7), and [M + 3] 394 (1.8, 1.8), [M + 4] 395 (0.2, 0.2). LCMS (+ESI): calcd for $C_{19}SiH_{23}O_7$ = 391.46, found 391.28, t_R = 20.90 min. ^{1}H NMR ($CDCl_3$,400 MHz): 1.20 (m, 2H), 2.5 (m, 2H), 3.8 (m, 2H), 6.3 (m, 2H), 7.5 (d, *J* = 7.5 Hz, 4H), 7.6 (d, *J* = 7.5 Hz, 4H). ^{13}C NMR ($CDCl_3$, 100 MHz): 10.0, 11.0, 12.0, 14.0, 26.0, 28.0, 48.0, 106, 126, 127.9, 129.3, 137.5, 156. The porphyrin group was not detected after the HF treatment.

Pheophorbide-Modified Fluorinated Glass (16). Pheophorbide monoester **12** reacted with 3-iodopropyltrimethoxysilane (0.50 mmol) and NaH (0.013 mmol) in THF. The THF was evaporated leaving a residue of pheophorbide **12** and 3-iodopropyltrimethoxysilane, which was added to toluene and 16 0.20 g Vycor caps **10**. The Vycor caps were dried at 350 °C prior to sensitizer attachment. Silane **12** was loaded in 0.17 μmol amounts (0.99% of the SiOH groups within a 0.08 mm depth) onto porous Vycor glass per cap and reached a penetration depth of 0.08 mm based upon microscopy experiments; thus, the sensitizer was largely confined to the outer face of the cap. Vycor **16** was stable in the dark; the sensitizer did not leach off to any measurable extent after washing with toluene or ethanol or after Soxhlet extraction with ethanol. In **16**, the ratio of fluorosilane to SiOH to sensitizer groups was 2666:100:0.7. FT-IR (λ, cm^{-1}): 4000−3500, 3030, 2960, 2483, 1730, 1408, 1254, 1080. UV (λ, air): 414 nm, 666 nm. Anal. Calcd: C, 0.576; H, 0.030; F, 0.152. Found: C, 0.531; H, 0.036; F, 0.369. After dissolution of solid **16** by the HF treatment, four main components were found. (i) Assigned to **A** based on GC/MS (EI +) calcd for $C_6SiH_4F_{12}$ = 332 g/mol, found 332 *m/z*, t_R = 5.59 min. ^{1}H NMR ($CDCl_3$, 400 MHz): 0.81 (t, $^3J_{^1H-^{19}F}$ = 25.2 Hz, $^4J_{^1H-^{19}F}$ = 0.4 Hz, 2H), 2.21 (m, $^3J_{^1H-^{19}F}$ = 25.2 Hz, $^4J_{^1H-^{19}F}$ = 0−4 Hz, 2H). ^{13}C NMR ($CDCl_3$, 100 MHz): 25.83, 51.09, 128.40, $^1J_{^{13}C-^{19}F}$ = 164.8 Hz, $^3J_{^{13}C-^{19}F}$ = 6.2 Hz, 128.50, $^1J_{^{13}C-^{19}F}$ = 164.8 Hz, $^3J_{^{13}C-^{19}F}$ = 6.2 Hz, 129.90, $^1J_{^{13}C-^{19}F}$ = 164.8 Hz, $^3J_{^{13}C-^{19}F}$ = 6.2 Hz, 130.00, $^1J_{^{13}C-^{19}F}$ = 64.8 Hz, $^3J_{^{13}C-^{19}F}$ =6.2 Hz. (ii) Assigned to **B** based on GC/MS (EI+) calcd for $C_{19}SiH_{23}O_7$ = 391, found 391, t_R = 8.93 min. LCMS (+ESI): calcd for $C_{19}SiH_{23}O_7$ = 391.46, found 391.29. ^{1}H NMR ($CDCl_3$,400 MHz): 1.15 (m, 2H), 3.2 (m, 2H), 4.8 (m, 2H), 6.3 (m, 2H), 7.5 (d, *J* = 7.5 Hz, 4H), 7.6 (d, *J* = 7.5 Hz, 4H). ^{13}C NMR ($CDCl_3$, 100 MHz): 10.0, 11.0, 12.0, 14.0, 26.0, 28.0, 48.0, 125.6, 128.49, 129.16, 129.93, 137.8, 138.63. (iii) Tentatively assigned to $CF_3CF_2CF_2CF_2CH_2CH_2Si(OH)_3$ (**C**) based on LCMS (+ESI) calcd for $C_6SiH_7O_3F_9$ = 326.00 g/mol, found 326.19 *m/z*, t_R = 15.35 min. ^{19}F NMR (200 MHz): −78.14 (3F), −113.21 (2F), −120.56 (2F), −122.45 (2F). (iv) Tentatively assigned to $HOCH_2C_6H_4OCH{=}CHOC_6H_4CH_2OCH_2CH_2CH_2Si$-$(F)_3$ (**D**) based on GC/MS (EI+) calcd for $C_{19}SiH_{20}O_4F_3$ = 398, found 399, t_R = 10.24 min. ^{19}F NMR (188 MHz): −112.6 (3F). The porphyrin group was not detected after the HF treatment.

dx.doi.org/10.1021/jo3006107 | J. Org. Chem. 2012, 77, 4557−4565

Ethene-Modified Glass (17). Compound **11** (3.4 mg, 0.0126 mmol) was added to 3-iodopropyltrimethoxysilane (0.250 mmol) and NaH (0.302 mg, 0.0126 mmol) in 5 mL of dry THF and the mixture refluxed at 70 °C for 24 h. The THF was evaporated under N_2 and was added to 100 mL of toluene and 2.4 mg of 60 μm Vycor particles (predried at 350 °C in a muffle furnace for 24 h) and refluxed at 110 °C for 24 h. The Vycor particles were washed by Soxhlet extraction with methanol for 24 h. In **17**, the ratio of SiOH to ethene groups was 0.02:100. FT-IR (λ, cm^{-1}): 4000−3500, 3080, 2960, 2420, 1750, 1360, 1200, 1055. UV (λ, air): transparent. Anal. Calcd: C, 0.037; H, 0.034. Found: C, 0.067; H, 0.024. After dissolution of solid **17** by the HF treatment, evidence suggested that **B** was liberated: GC/MS (EI+) calcd for $C_{19}SiH_{23}O_7$ = 391, found 391, t_R = 8.925 min. LCMS (+ESI): calcd for $C_{19}SiH_{23}O_7$ = 391.20 found 391.28515, t_R = 20.92 min. ^{1}H NMR ($CDCl_3$,400 MHz): 1.20 (m, 2H), 2.5 (m, 2H), 3.8 (m, 2H), 6.3 (m, 2H), 7.5 (d, J = 7.5 Hz, 4H), 7.6 (d, J = 7.5 Hz, 4H). ^{13}C NMR ($CDCl_3$, 100 MHz): 10.0, 11.0, 12.0, 14.0, 26.0, 28.0, 48.0, 125.6, 128.49, 129.16, 129.93, 137.8. ^{1}H NMR ($CDCl_3$,400 MHz): 1.20 (m, 2H), 2.5 (m, 2H), 3.8 (m, 2H), 6.3 (m, 2H), 7.5 (d, J = 7.5 Hz, 4H), 7.6 (d, J = 7.5 Hz, 4H). ^{13}C NMR ($CDCl_3$, 100 MHz): 10.0, 11.0, 12.0, 14.0, 26.0, 28.0, 48.0, 106, 126, 127.9, 129.3, 137.5, 138.9.

Ethene-Modified Fluorinated Glass (18). In **18**, the ratio of fluorosilane to SiOH to ethene groups was 2666:100:0.7. FT-IR (λ, cm^{-1}): 4000−3500, 3030, 2960, 2483, 1730, 1408, 1254, 1080. UV (λ, air): transparent. Anal. Calcd: C, 0.576; H, 0.030; F, 1.368. Found: C, 1.075; H, 0.065; F, 1.399. After dissolution of solid **18** by the HF treatment, three main components were found. (i) Assigned to **A** based on GC/MS (EI+) calcd for $C_6SiH_4F_{12}$ = 332 g/mol, found 332, m/z, t_R =5.56 min. ^{1}H NMR ($CDCl_3$, 400 MHz): 0.8 (t, $^3J_{H-^{19}F}$ = 46.7 Hz, $^4J_{H-^{19}F}$ = 0−4 Hz, 2H), 2.2 (m, $^3J_{H-^{19}F}$ = 46.7 Hz, $^4J_{H-^{19}F}$ = 0−4 Hz, 2H). ^{13}C NMR ($CDCl_3$, 100 MHz): 21.40, 50.22, 128.40, $^1J_{^{13}C-^{19}F}$ = 164.8 Hz, $^3J_{^{13}C-^{19}F}$ = 6.2 Hz, 129.50, $^1J_{^{13}C-^{19}F}$ = 164.8 Hz, $^3J_{^{13}C-^{19}F}$ = 6.2 Hz, 129.90, $^1J_{^{13}C-^{19}F}$ = 164.8 Hz, $^3J_{^{13}C-^{19}F}$ = 6.2 Hz, 130.30, $^1J_{^{13}C-^{19}F}$ = 164.8 Hz, $^3J_{^{13}C-^{19}F}$ = 6.2 Hz. (ii) Assigned to **B** based on GC/MS (EI+) calcd for $C_6SiH_7O_3F_9$ = 326.00 g/mol, found 326.1939700 m/z, t_R =15.35 min. LCMS (+ESI): calcd for $C_{19}SiH_{23}O_7$ = 391.46, found 391.29. ^{1}H NMR ($CDCl_3$,400 MHz): 1.20 (m, 2H), 2.5 (m, 2H), 3.8 (m, 2H), 6.3 (m, 2H), 7.5 (d, J = 7.5 Hz, 4H), 7.6 (d, J = 7.5 Hz, 4H). ^{13}C NMR ($CDCl_3$, 100 MHz): 10.0, 11.0, 12.0, 14.0, 26.0, 28.0, 48.0, 106, 126, 127.9, 129.3, 137.5, 156. GC/MS (EI+): calcd for $C_{19}SiH_{23}O_7$ = 391, found 391, t_R = 9.00 min. (iii) Tentatively assigned to **C** based on LCMS (+ESI) calcd for $C_{19}SiH_{20}O_4F_3$ = 398.44, found 397.25.

Photocleavage Procedure. Oxygen gas and 669 nm excitation light were delivered through the fiber optic to probe tips **15** and **16**, which were inserted into two types of media: (1) homogeneous toluene-d_8 solution (1.0 mL) and (2) bovine muscle tissue purchased at a local supermarket was assumed to have been aged at 0 °C for 1−3 days. The photocleavage of sensitizer **3** away from the probe tip was followed by UV−vis in toluene-d_8 solution and by fluorescence spectroscopy (λ_{ex} = 416 nm) in the bovine tissue at room temperature. The tissue was used within 2 days of purchase. Cylindrical cores (ea. Ten mm/5 g) were cut for removal of a tissue disk using a sterile cork borer of 5 mm diameter, placed in Petri dishes, where the probe tip was embedded into the center of the disk. After fiberoptic irradiation and sensitizer deposition, discs were cut in the direction of the muscle fibers resulting in six samples containing various amounts of photocleaved sensitizer **3**. The pigmentation of photocleaved sensitizer **3** was greatest near the cap and decreased a distance of 3 mm from the probe tip as measured with the postprocessing software. Toughness and tenderness were not assessed after the fiberoptic treatment. The hydrolysis of **3** to give the 4-hydroxybenzylic alcohol and formic acid was not examined in the two types of media.

The amount photoreleased was calculated as follows: % photorelease **3** = [(photorelease/loading per area)] × 100; % conversion = [(photorelease + adsorbed per area/loading per area)] × 100; % adsorbed **3** = [(adsorbed per area/loading per area)] × 100. A ∼10% portion of the upper rim of the fiber tip was shielded from light. Thus, the quantity of dye that photocleaved was based on ∼90% of the cap area exposed to the light. UV−vis experiments showed no evidence of bleaching of the photoreleased sensitizer **3**.

k_T Measurements. A 10 Hz Nd:YAG Q-switched laser was used producing 355 nm, ∼4 ns fwhm, and 1−3 mJ/pulse. The singlet oxygen lifetime and k_T kinetic measurements were determined using a photomultiplier tube at an operating voltage of −650 V. Mixtures of 10 to 50 g/L quantities of Vycor particles **6**, **10**, **17**, or **18** were immersed individually in 3.0 mL toluene-h_8. The particle−toluene slurries were irradiated with the Nd:YAG pulsed laser at λ_{ex} = 355 nm, and contained sensitizer **4** (5.3×10^{-4} M) and were stirred with a microstir bar with O_2 flowing (60 mL/h). The $^1O_2$ luminescence intensity was monitored through a NIR bandpass filter centered at 1270 nm (OD4 blocking, fwhm = 15 nm). Bandpass filters centered at 1220 and 1315 nm were also employed and verified minute intensities compared to 1270 nm, but subtractions of the signals was not performed. The $^1O_2$ luminescence signals were registered on a 600 MHz oscilloscope and the kinetic data for the lifetime was determined by a least-squares curve-fitting procedure.

Calculations. The number of "moles" of silanol per gram Vycor was estimated from the surface area (250 m^2/g) and the presence of four silanol sites per 100 Å^2. Dividing the surface area by 1×10^{-18} m^2 gave $2.5 \times 10^{20} \times 4 = 1 \times 10^{21}$ silanol sites per gram Vycor. The number of silanol sites per gram was then converted to moles by dividing by Avogadro's number to give 1.6×10^{-3} moles of silanol per gram. The area of silane intruded glass in Å^2 is given in eq 1. The area occupied by four molecules on the Vycor surface at a given loading of sensitizersilane, fluorosilane, ethenesilane is given by eq 2. The molecule−molecule distance on the PVG surface is given by eq 3. The calculation of the mass percent of the fluorosilane, sensitizersilane, and ethenesilane covalently was done as the amount (in grams) of each silane covalently attached divided by one gram of Vycor ×100. The amount in grams was calculated from the number of moles of the silane loaded onto the Vycor.

$$\text{glass area (Å}^2\text{)} = \frac{(\text{mol SiOH}) \times (6.023 \times 10^{23}\ \text{SiOH groups/mol}) \times (100\ \text{Å}^2)}{4\ \text{SiOH groups}} \quad (1)$$

$$\text{area between 4 molecule sites (Å}^2\text{)} = \frac{(\text{glass area} \times 4)}{\text{number of molecules}} \quad (2)$$

$$\text{distance between molecules (Å)} = \sqrt{(\text{area of 4 molecules Å}^2)} \quad (3)$$

■ ASSOCIATED CONTENT

Ⓢ Supporting Information

Photographs of the fiber tips and of tip **16** in contact with bovine tissue. Absorption and FT-IR spectra of **6**, **10**, and **15**−**18**. GC/MS, LCMS, and ^{1}H, ^{13}C, and ^{19}F NMR spectra of small molecules arising from the HF treatment of glasses **10** and **15**−**18**. This material is available free of charge via the Internet at http://pubs.acs.org.

■ AUTHOR INFORMATION

Corresponding Author

*E-mail: agreer@brooklyn.cuny.edu.

■ ACKNOWLEDGMENTS

We acknowledge support from the National Institute of General Medical Sciences (NIH SC1GM093830). We thank Stanley Kimani for discussions and Zhong Wang of the Hunter College Bio-Imaging Facility and Mim Nakarmi of the Brooklyn College Physics Department for use of requisite equipment. We also thank Alison Domzalski for the photography work and Leda Lee for the graphic arts work.

REFERENCES

(1) Kessel, D.; Foster, T. H., Eds. Symposium-In-Print: Photodynamic therapy. *Photochem. Photobiol.* **2007**, *83*, 995−1282.
(2) Zamadar, M.; Ghosh, G.; Mahendran, A.; Minnis, M.; Kruft, B. I.; Ghogare, A.; Aebisher, D.; Greer, A. *J. Am. Chem. Soc.* **2011**, *133*, 7882−7891.
(3) Mahendran, A.; Kopkalli, Y.; Ghosh, G.; Ghogare, A.; Minnis, M.; Kruft, B. I.; Zamadar, M.; Aebisher, D.; Davenport, L.; Greer, A. *Photochem. Photobiol.* **2011**, *87*, 1330−1337.
(4) Matsumoto, M.; Suzuki, H.; Watanabe, N.; Ijuin, H. K.; Tanaka, J.; Tanaka, C. *J. Org. Chem.* **2011**, *76*, 5006−5017.
(5) Bartlett, P. D.; Baumstark, A. L.; Landis, M. E. *J. Am. Chem. Soc.* **1974**, *96*, 5557.
(6) Adam, W.; Arnold, M. A.; Saha-Moeller, C. R. *J. Org. Chem.* **2001**, *66*, 597−604.
(7) Zaklika, K. A.; Burns, P. A.; Schaap, A. P. *J. Am. Chem. Soc.* **1978**, *100*, 318−320.
(8) Xu, L.; Karunakaran, R. G.; Guo, J.; Yang, S. *ACS Appl. Mater. Interfaces* **2012**, *4*, 1118−1125.
(9) Cho, W. K.; Kang, S. M.; Kim, D. J.; Yang, S. H.; Choi, I. S. *Langmuir* **2006**, *22*, 11208−11213.
(10) El-Nahhal, I. M.; El-Ashgar, N. M. *J. Organomet. Chem.* **2007**, *692*, 2861−2886.
(11) Nakajima, A.; Hashimoto, K.; Watanabe, T.; Takai, K.; Yamauchi, G.; Fujishima, A. *Langmuir* **2000**, *16*, 7044−7047.
(12) Singh, R. P.; Way, J. D.; McCarley, K. C. *Ind. Eng. Chem. Res.* **2004**, *43*, 3033−3040.
(13) Mello, R.; Martínez-Ferrer, J.; Alcalde-Aragonés, A.; Varea, T.; Acerete, R.; Gonzaléz-Núñez, M. E.; Asensio, G. *J. Org. Chem.* **2011**, *76*, 10129−10139.
(14) Kidder, M. K.; Chaffee, A. L.; Nguyen, M.-H. T.; Buchanan, A. C., III. *J. Org. Chem.* **2011**, *76*, 6014−6023.
(15) Baumstark, A. In *Advances in Oxygenated Processes*; JAI Press: Greenwich, CT, 1988; Vol. *1*, pp 31−84.
(16) MacManus-Spencer, L. A.; Edhlund, B. L.; McNeill, K. *J. Org. Chem.* **2006**, *71*, 796−799.
(17) Murthy, R. M.; Bio, M.; You, Y. *Tetrahedron Lett.* **2009**, *50*, 1041−1044.
(18) Ciscato, L. F. M. L.; Bartoloni, F. H.; Weiss, D.; Beckert, R.; Baader, W. J. *J. Org. Chem.* **2010**, *75*, 6574−6580.
(19) Jiang, M. Y.; Dolphin, D. *J. Am. Chem. Soc.* **2008**, *130*, 4236−4237.
(20) Baugh, S. D. P.; Yang, Z.; Leung, D. K.; Wilson, D. M.; Breslow, R. *J. Am. Chem. Soc.* **2001**, *123*, 12488−12494.
(21) Jensen, R. L.; Arnbjerg, J.; Ogilby, P. R. *J. Am. Chem. Soc.* **2010**, *132*, 8098−8105.
(22) Gorman, A. A.; Lovering, G.; Rodgers, M. A. J. *J. Am. Chem. Soc.* **1979**, *101*, 3050−3055.
(23) Gorman, A. A.; Gould, I. R.; Hamblett, I. *J. Am. Chem. Soc.* **1982**, *101*, 7098−7104.
(24) Erden, I.; Ergonenc Alscher, P.; Keeffe, J. R.; Mercer, C. *J. Org. Chem.* **2005**, *70*, 4389−4392.
(25) Zamadar, M.; Greer, A. Singlet Oxygen as a Reagent in Organic Synthesis. In *Handbook of Synthetic Photochemistry*; Albini, A., Fagnoni, M., Eds.; Wiley-VCH: Weinheim, 2010; pp 353−386.
(26) Higgins, R.; Foote, C. S.; Cheng, H. In *Advances in Chemistry Series*; Gould, R. F., Ed.; American Chemical Society: Washington, DC, 1968; Vol. *77*, pp 102−117.
(27) Hall, J. F. B.; Han, X.; Poliakoff, M.; Bourne, R. A.; George, M. W. *Chem. Commun.* **2012**, *48*, 3073−3075.
(28) Cojocaru, B.; Laferrière, M.; Carbonell, E.; Parvulescu, V.; García, H.; Scaiano, J. C. *Langmuir* **2008**, *24*, 4478−4481.
(29) Pace, A.; Pierro, P.; Buscemi, S.; Vivona, N.; Clennan, E. L. *J. Org. Chem.* **2007**, *72*, 2644−2646.
(30) Pace, A.; Clennan, E. L. *J. Am. Chem. Soc.* **2002**, *124*, 11236−11237.
(31) Jockusch, S.; Sivaguru, J.; Turro, N. J.; Ramamurthy, V. *Photochem. Photobiol. Sci.* **2005**, *4*, 403−405.
(32) Simon, V.; Devaux, C.; Darmon, A.; Donnet, T.; Thiénot, E.; Germain, M.; Honnorat, J.; Duval, A.; Pottier, A.; Borghi, E.; Levy, L.; Marill, J. *Photochem. Photobiol.* **2010**, *86*, 213−222.
(33) Chin, K. K.; Trevithick-Sutton, C. C.; McCallum, J.; Jockusch, S.; Turro, N. J.; Scaiano, J. C.; Foote, C. S.; Garcia-Garibay, M. A. *J. Am. Chem. Soc.* **2008**, *130*, 6912−6913.
(34) Li, Y.; Zhang, J.; Zhu, S.; Dong, H.; Jia, F.; Wang, Z.; Tang, Y.; Zhang, L.; Zhang, S.; Yang, B. *Langmuir* **2010**, *26*, 9842−9847.
(35) Clennan, E. L.; Noe, L. J.; Wen, T.; Szneler, E. *J. Org. Chem.* **1989**, *54*, 3581−3584.
(36) Celaje, J. A.; Zhang, D.; Guerrero, A. M.; Selke, M. *Org. Lett.* **2011**, *13*, 4846−4849.
(37) Schmidt, R.; Brauer, H.-D. *J. Am. Chem. Soc.* **1987**, *109*, 6976−6981.
(38) Ogilby, P. R.; Foote, C. S. *J. Am. Chem. Soc.* **1983**, *105*, 3423.
(39) Hurst, J. R.; Schuster, G. B. *J. Am. Chem. Soc.* **1983**, *105*, 5756.
(40) Rodgers, M. A. J. *J. Am. Chem. Soc.* **1983**, *105*, 6201.
(41) Sivaguru, J.; Solomon, M. R.; Poon, T.; Jockusch, S.; Bosio, S. G.; Adam, W.; Turro, N. J. *Acc. Chem. Res.* **2008**, *41*, 387−400.
(42) Schmidt, R. *J. Am. Chem. Soc.* **1989**, *111*, 6983−6987.
(43) Lancaster, J. R.; Martí, A. A.; López-Gejo, J.; Jockusch, S.; O'Connor, N.; Turro, N. J. *Org. Lett.* **2008**, *10*, 5509−5512.
(44) Clennan, E. L.; Chen, M. F. *J. Org. Chem.* **1995**, *60*, 6004−6005.
(45) Wilkinson, F.; Helman, W. P.; Ross, A. B. *J. Phys. Chem. Ref. Data* **1995**, *24*, 663−1021.
(46) Ytzhak, S.; Wuskell, J. P.; Loew, L. M.; Ehrenberg, B. *J. Phys. Chem. B* **2010**, *114*, 10097−10104.
(47) Ben-Dror, S.; Bronshtein, I.; Wiehe, A.; Röder, B.; Senge, M. O.; Ehrenberg, B. *Photochem. Photobiol.* **2006**, *82*, 695−701.
(48) Mir, Y.; van Lier, J. E.; Paquette, B.; Houde, D. *Photochem. Photobiol.* **2008**, *84*, 1182−1186.
(49) Chen, Q.; Huang, Z.; Chen, H.; Shapiro, H.; Beckers, J.; Hetzel, F. W. *Photochem. Photobiol.* **2002**, *76*, 197−203.
(50) Ogilby, P. R. *Chem. Soc. Rev.* **2010**, *39*, 3181−3209.
(51) Hamblin, M. R.; Miller, J. L.; Rizvi, I.; Loew, H. G.; Hasan, T. *Br. J. Cancer* **2003**, *89*, 937−943.
(52) Mello, R.; Olmos, A.; Varea, T.; Gonzaléz-Núñez, M. E. *Anal. Chem.* **2008**, *80*, 9355−9359.
(53) Marans, N. S.; Sommer, L. H.; Whitmore, F. C. *J. Am. Chem. Soc.* **1951**, *73*, 5127−5130.